ISSN 0869-5938, Stratigraphy and Geological Correlation, 2015, Vol. 23, No. 3, pp. 246–261. © Pleiades Publishing, Ltd., 2015.
Original Russian Text © A.V. Kuptsova, A.K. Khudoley, W. Davis, R.H. Rainbird, A.V. Molchanov, 2015, published in Stratigrafiya. Geologicheskaya Korrelyatsiya, 2015, Vol. 23, No. 3, pp. 13–29.

Results of the U-Pb Age of Detrital Zircons from Upper Proterozoic Deposits of the Eastern Slope of the Anabar Uplift

A. V. Kuptsova[a], A. K. Khudoley[a], W. Davis[b], R. H. Rainbird[b], and A. V. Molchanov[c]

[a] *St. Petersburg State University, St. Petersburg, 199034 Russia*
e-mail: alina-kuptsova@yandex.ru
[b] *Geological Survey of Canada, Ottawa, Canada*
[c] *Karpinsky Russian Geological Research Institute (VSEGEI), Sredny pr. 74, St. Petersburg, 199106 Russia*

Received December 26, 2012; in final form, August 25, 2014

Abstract—The Upper Proterozoic sequence in the southern part of the East Anabar Basin, as throughout the entire framing of the Anabar uplift, has a two-unit terrigenous-carbonate structure. The results of the U-Pb dating of detrital zircons show that there is a difference in stratigraphy of Riphean strata in the north and south of the Anabar Uplift. In the north, deposits of the entire sequence are regarded as Early Riphean; in the south, the thickness of these deposits is reduced to 70 m. The overlying stratum is regarded as Upper Riphean–Vendian. As the strata in the southern part of the East Anabar Basin strata are of younger (Late Riphean–Vendian) age, they cannot be assigned to the Mukun and Billyakh groups. The Riphean–Vendian deposits accumulated mainly through erosion of crystalline rocks of the Anabar Uplift. In the upper part of the sequence, the Vendian magmatic complexes located probably within the Taimyr Orogen played a significant role as provenance areas.

Keywords: Riphean, provenance areas, geochronology, Mukun Group, Anabar Uplift
DOI: 10.1134/S0869593815030053

INTRODUCTION

The sequence of Riphean deposits in the framing of the Anabar Uplift, a reference section in the Siberian Platform, is characterized by a significant thickness (*Opornyi...*, 1970; Semikhatov and Serebryakov, 1983; *Stratigrafiya...*, 2005). The composition of deposits and their stratigraphy were studied during the geological mapping in the 1960s–1970s (*Gosudarstvennaya...*, 1983), as well as during subsequent sedimentological (Petrov, 2011), paleontological (Sergeev, 1993; Sergeev et al., 2007), and isotope-geochronological (mainly, K-Ar and Rb-Sr) studies (Gorokhov et al., 1991, 2001). At the same time, there is a lack of information on the provenance areas and evolution of the Riphean sedimentary basins on the western and eastern slopes of the Anabar uplift.

The main objective of our study was to investigate the provenance areas and to clarify the stratigraphy of Upper Proterozoic complexes in the southern part of the East Anabar Basin by the U-Pb zircon dating.

GEOLOGICAL STRUCTURE OF THE ANABAR UPLIFT REGION: A REVIEW

According to modern concepts, the Anabar Shield basement has block structure (Rozen, 1995; Rozen et al., 2006; *Tektonika...*, 2001; Molchanov et al., 2003; Smelov and Timofeev, 2007). The western and central parts of the Anabar Shield are mainly composed of Archean granulite-gneiss Daldyn and Magan terranes; the eastern part comprises the Birektin granite-greenstone terrane (Fig. 1), which is mainly composed of Early Proterozoic metacarbonates and metagraywackes of the Khapchan belt (Rosen et al., 2000).

Terranes are separated by submeridional melange zones (*Tektonika...*, 2001; Smelov and Timofeev, 2007) or tectonic fluid zones according to the terminology by Molchanov (2004). The largest of these zones are Kotuikan-Monkhool and Billyakh. The first zone separates the Magan and Daldyn terranes; the second one, the Daldyn terrane and Khapchan zone (Fig. 1).

Riphean terrigenous and carbonate rocks, widely distributed in the framing of the Anabar Shield, are underlain with a sharp angular unconformity by the weathering crust of the Archean–Lower Proterozoic basement and are overlain by Vendian–Cambrian platform formations (Fig. 1). Despite the structural similarities in sequences of Riphean sedimentary complexes on the western and eastern slopes on the Anabar uplift, significant variations in the composition and thicknesses allow one to suggest that their accumulation occurred in different sedimentation basins: West Anabar and East Anabar.

The structural pattern of these basins is apparently determined by their confinement to the Fomich–Kotui (Surkov and Grishin, 1997) and Udzha aulacogenes, respectively (*Tektonika...*, 2001; Gladkochub et al.,

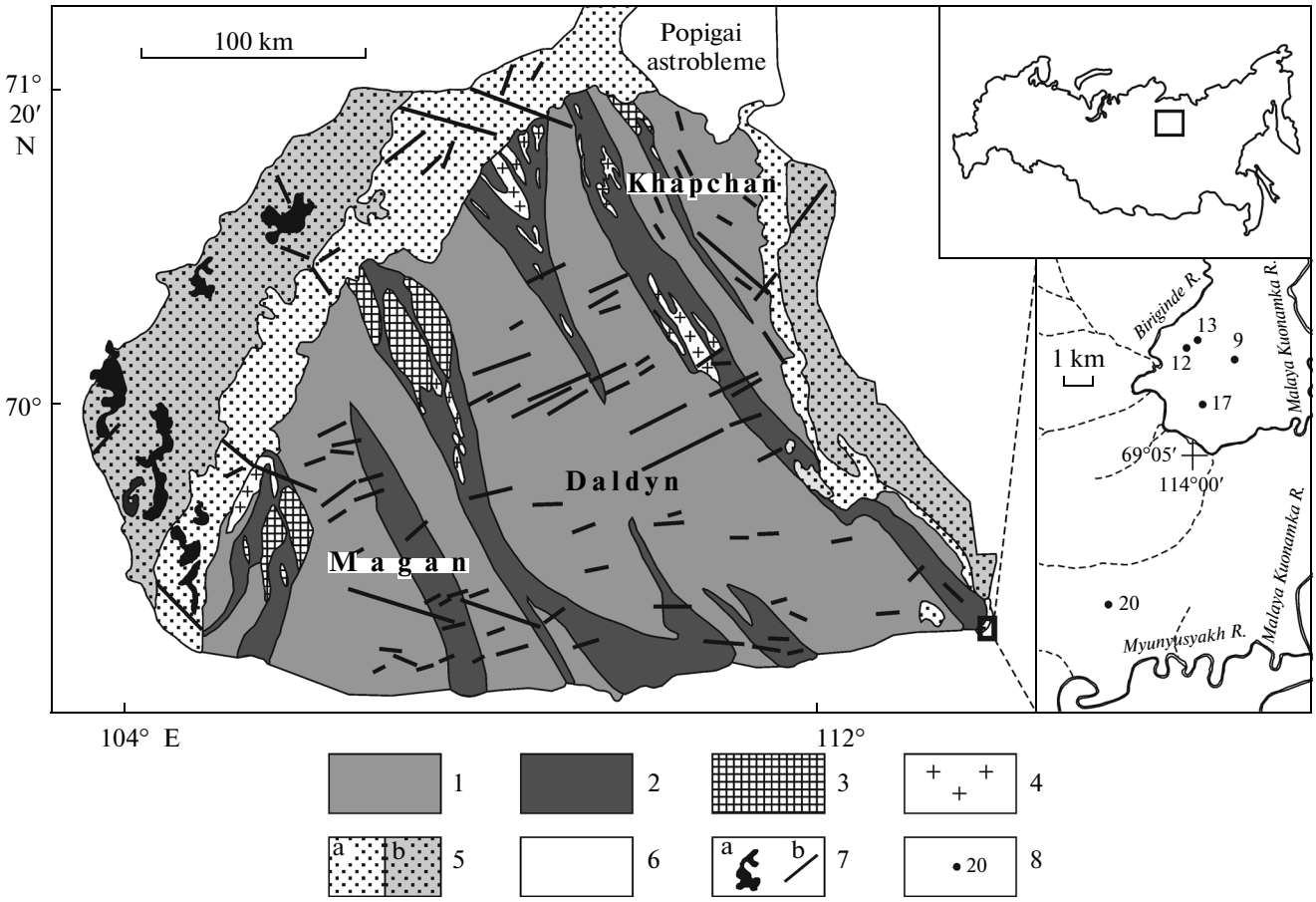

Fig. 1. Scheme of geological structure of the Anabar Shield and locality sites of sample wells in the southern part of the East Anabar Basin (*Gosudarstvennaya...*, 1983; Rozen, 1995; Surkov and Grishin, 1997). (1) Archean–Proterozoic terrains and belts (Magan, Daldyn, Khapchan); (2) Early Proterozoic mélange zones (Kotuikan-Monkhool, Billyakh, etc.); (3, 4) Early Proterozoic intrusions of anorthosites (3) and granitoides (4); (5, 6) sedimentary cover: (5) Early Riphean deposits of the Mukun (a) and Billyakh (b) groups, (6) Vendian–Paleozoic deposits; (7) Riphean–Triassic magmatic complexes: (a) dolerite sills, (b) basite dikes; (8) number and location site of well. Area of study is outlined by rectangle.

2009). The relations between these basins are still debatable, since they are geographically separated by Paleozoic complexes and the Cenozoic Popigai impact structure (astrobleme) in the north, whereas on the southern slope of the Anabar Shield the Riphean deposits are absent and the crystalline basement is overlapped by Vendian deposits (*Gosudarstvennaya...*, 1983; *Tektonika...*, 2001).

The thickness of Riphean deposits in the East Anabar Basin is no less than 500 m, increasing to 1–2 km in an easterly direction, according to the geophysical data (Surkov and Grishin, 1997; *Tektonika* ..., 2001). The sequence of Riphean deposits on the eastern slope is divided into two groups: Mukun (terrigenous) and Billyakh (terrigenous-carbonate).

The basal part of the Mukun Group, the total thickness of which in the East Anabar Basin does not exceed 250 m, is represented by large- to medium-grained, horizontally and cross-stratified red quartz-feldspar sandstones and conglomerates and, higher in the section, by gray less coarse grained more matured quartz rocks. The deposits of the Mukun Group are conformably overlain by carbonate rocks of the Billyakh Group that are distinguished by the first occurrence of stromatolite dolomites. The Billyakh Group (about 300 m) comprises two formations: Kotuikan, composed of interbedded dolomites, sandstones and siltstones, and Yusmastakh, composed of coarse-fragmental lower strata and mainly dolomite upper strata (*Gosudarstvennaya...*, 1983; *Stratigrafiya...*, 2005).

In the north of the East Anabar Basin, the lower part of the Yusmastakh Formation is intruded by a dike, whose baddeleyite U-Pb age is 1384 ± 2 Ma (Ernst et al., 2000). This gives us grounds to assume that all or, at least, the greater part of the Billyakh Group has Early Riphean age. In the Fomich River basin (the northern part of the West Anabar Basin), the contact zone of the Mukun and Billyakh groups is intruded by a sill with Sm-Nd isochrone age of 1513 ± 51 Ma and baddeleyite U-Pb age of 1493 ± 34 Ma. These age data indicate that the age of rocks of the

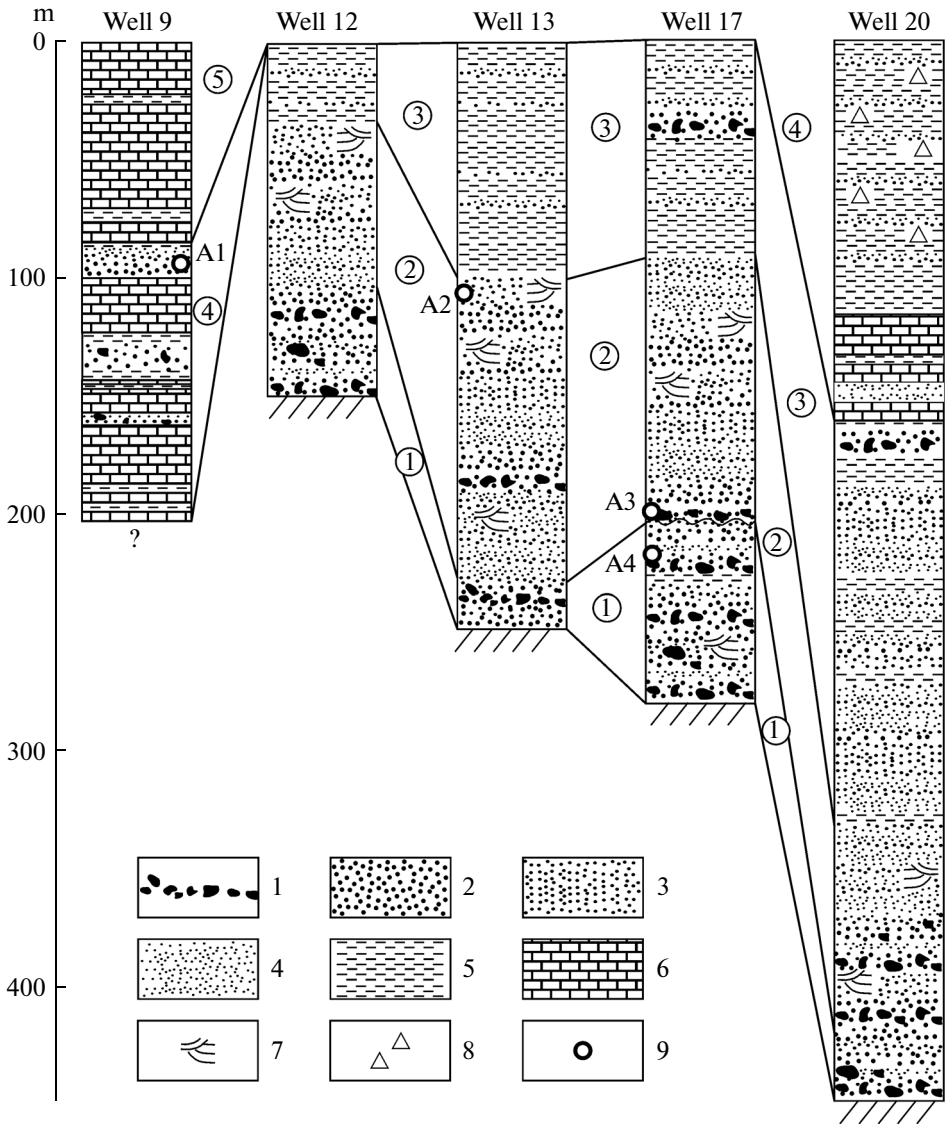

Fig. 2. Map showing sample locations and correlation scheme of well sections drilled in the southern part of the East Anabar Basin. (1) Conglomerates and gravelites; (2) coarse sandstones; (3) average-grained sandstones; (4) fine and ultrafine sandstones; (5) siltstones and claystones; (6) dolomites; (7) horizontally and cross-stratified structures; (8) brecciated zone; (9) locality sites of samples for U-Pb age dating of detrital zircons.

Mukun Group is about 1500 Ma (Veselovskii et al., 2006; Khudoley et al., 2009).

LITHOLOGY OF TERRIGENOUS RIPHEAN–VENDIAN ROCKS

The area of study was located in the southern part of the East Anabar Basin (the basins of Myunyusyakh, Biriginde, and Malaya Kuonamka rivers). The sequence of Riphean deposits was studied in core sections of five wells (Fig. 1), which were drilled by Amakinskaya GSE (ALROSA). The section was previously correlated with the Mukun and Billyakh groups of Riphean deposits, whereas the uppermost part of the section was correlated with the Vendian Starorechenskaya Group. The sequence was divided into five strata on the basis of lithological features (Fig. 2).

The lower part of the Riphean–Vendian section in the southern part of the East Anabar Basin is made of gravellites, conglomerates, quartz-feldspar sandstones with relic cross-bedding (stratum 1 in Fig. 2). Stratum 1 was identified in all wells (except for Borehole 9, where this stratum is not opened). The total thickness varies from 18–19 m in boreholes 13 and 20 to 93.7 m in Borehole 17.

Conglomerates and grits lie directly on the weathered crust of the crystalline basement, whose outwash material often occurs at the base of deposits. Conglomerates are composed of well-rounded pebbles of quartz, strongly altered feldspar fragments, and quartz-

feldspar metasomatites, cemented by different-sized sandstone.

The main part of the section is represented by an alternation of predominantly coarse-grained red sandstones with large pebbles of quartz, gravel sandstone, quartz grit, and conglomerate. The rock structure is cross-stratified with alternation of layers of different-sized grits. Stratum 1 comprises several rhythms a few tens of meters thick. From bottom to top of a rhythm, conglomerates or grits are followed by sandstones and siltstones. At the bases of rhythms, there are indistinct erosion surfaces.

The clastic fraction of the sandstone is predominantly made of quartz (40–80%), feldspar (20–40%), and fragments of quartzite, gneiss, and altered metabasites (10%). The accessory minerals are magnetite, ilmenite, rutile, leucoxene, glauconite, apatite, and zircon. Most of the fragments are angular to rounded, and poorly sorted, which indicates proximity of a provenance area. A high degree of roundness of single rock fragments suggests that they originated from older sediments and were involved in several cycles of sedimentation.

Coarse-grained sandy-gravel composition, inconsistent sedimentary bodies in strike and thickness, numerous erosional surfaces, and cross-bedding are evidence of alluvial-deltaic origin of stratum 1, probably in a network of branched streams and alluvial cones.

Higher in the section is the strata of massive, rarely platy inequigranular sandstones with rare interbedded conglomerates, gravellites, and siltstones (stratum 2 in Fig. 2). The total thickness of the stratum varies from 50 m in Borehole 12 to 95 m in Borehole 17. Stratum 2 was identified in all wells (except for Borehole 9, where it was not opened).

Stratum 2 is characterized by horizontally and cross-stratified structure. Angular, poorly rounded rock fragments dominate. However, there are very well rounded quartz grains. Deposits are poorly sorted in general, while there are rare bands of well-sorted quartz sandstones.

The clastic fraction of the sandstone is dominated by quartz (93–60%); feldspar (7–45%) and rock fragments up to (10%) are in a subordinate amount. Rock fragments are cemented by fine-grained quartz-feldspar aggregate, illite, and less commonly calcite and dolomite. Accessory minerals often form small lenses of natural black concentrates made of magnetite, ilmenite, biotite, zircon, apatite, tourmaline, pyrite, and less commonly sphene. Over the entire section are single thin layers containing grains of glauconite.

The predominance of horizontally and cross-stratified sandstones, interlayers enriched in heavy minerals similar to natural black concentrates, grains of glauconite, and structures resembling wave ripple marks indicate that formation of stratum 2, as well as of the overlying strata, occurred in a coastal marine environment under a decreasing role of temporary streams supplying unsorted coarse-grained material.

The above-lying stratum 3 (Fig. 2) is composed mainly of rhythmically alternating medium-grained sandstones, variegated siltstones, and mudstones with rare layers and lenses of gravellites and gray fine-grained clayey dolomites. The thickness of the stratum is about 97 m on average, reaching 155 m in the section of Borehole 20. The minimum thickness (30 m) was recorded in the Borehole 12. Stratum 3 was identified in all wells (except for Borehole 9, where it was not opened).

Sandstones vary from quartz to arkose in mineral composition. In general, graded bedding is observed. The main proportion of fragments is represented by quartz (93–55%), feldspar (40–7%), and rock fragments (3%). Sandstones are poorly sorted with angular-rounded fragments. The cement of quartz sandstones is regenerated quartz, illite-muscovite, and less commonly carbonate and ferruginous.

Sandstones are characterized by horizontal and cross-bedding; siltstones and mudstones, by thin horizontal and irregular wavy bedding and desiccation cracks. Consedimentational folds and microfaults are locally developed owing to deformation of the nonlithified sediment. The matrix of the mudstone is often made of carbonized clay material with a varying amount (5–30%) of chloritized biotite plates and sandy-sized rock fragments.

The next stratum (stratum 4 in Fig. 2) is composed of interbedded coarse light dolomites (in predominance) and sandstones (in subordinate amount), as well as siltstones and mudstones. A distinctive feature of terrigenous rocks of this stratum is occurrence of carbonates in the clastic fraction. There are thin layers of stromatolite dolomite and sandy dolomite with a high content of quartz grains. Sometimes, dolomites have desiccation cracks and brecciation zones. Sandstones are gray, quartz, small- and medium-grained, with thin lenses of quartz gravellites and pebble conglomerates. The relic cross-bedding is manifested. Among pebbles are dolomite fragments. Stratum 4 is recorded only in boreholes 9 and 20, where its thickness is about 150 m (Fig. 2).

Higher in the section, the proportion of terrigenous material sharply decreases. The stratum is crowned by light gray silicified stromatolite dolomites (strata 5 in Fig. 2).

METHODS

In order to reconstruct the history of formation of Upper Precambrian sedimentary strata of the southern part of the East Anabar Basin, the U-Pb dating of detrital zircons was performed. Four representative samples were petrographically selected from more than 90 samples collected in different parts of the section (Fig. 2). Sample A4 was collected in the conglomerate unit (strata 1) from the lower part of the terrige-

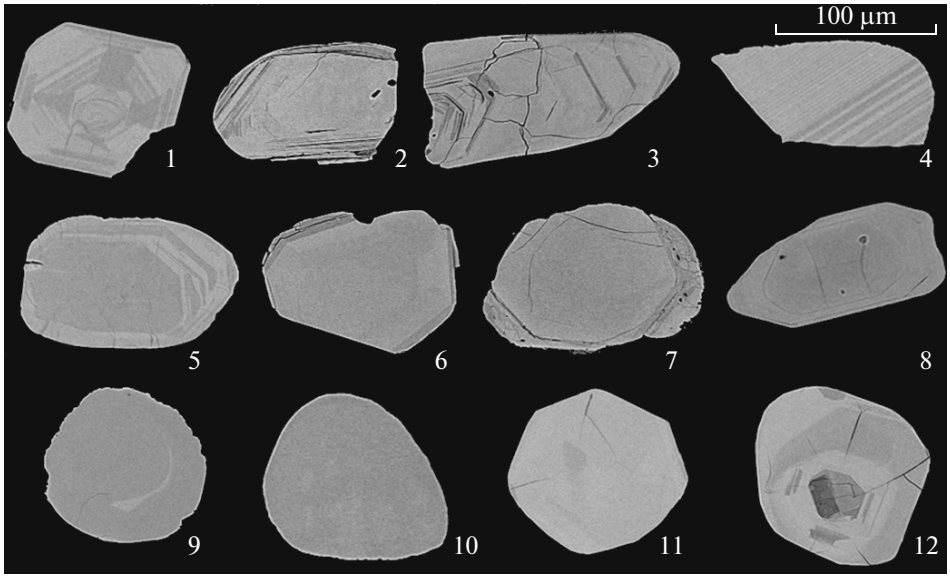

Fig. 3. Morphology and structure of zircon grains from sandstones of the southern part of the East Anabar Basin.

nous section (depth of 217.5 m, Borehole 17). Sample A3 was collected in the same well at a depth of 205.3 m. This sample characterizes one of the sandstone units, overlying a conglomerate interbed with indistinct signs of erosion at the base. We consider this unit as a base of stratum 2, although the underlying rocks of stratum 1 in this section are quite similar to those of stratum 2 in composition and structure. Sample A2 was collected in the upper part of the sandstone stratum 2, opened at a depth of 105 m in Borehole 13, stratigraphically above Sample A3. Sample A1 was collected in the upper part of the mudstone-dolomite stratum 4 at a depth of 87.8 m in Borehole 9, approximately 2.5 m below the unconformity contact with Vendian dolomites.

Zircons were selected using a standard method at the Institute of Precambrian Geology and Geochronology, Russian Academy of Sciences (St. Petersburg). The least broken cores of zircon grains were dated. In order to select sites for age dating, zircon grains were studied under a Zeiss Evo 50 scanning electron microscope. The U-Pb (SHRIMP-II) zircon grains were dated at the Geological Survey of Canada (Ottawa) following the procedure described in detail in (Stern, 1997; Stern and Amelin, 2003), using an internal standard z6266 with $^{206}Pb/^{238}U$ age of 559 Ma. The intensity of the primary beam of negative molecular ions of oxygen was 5–6.5 nA at a crater 25 μm in diameter. Each analysis represents the average of five scans. The error of zircon U-Pb ages was $\pm 1\sigma$. The results obtained were processed using the programs of SQUID2 and Isoplot 3.0 (Ludwig, 2000, 2003). All the isotopic U-Pb zircon age datings are given in the table.

When studying detrital zircons, the age calculated by the $^{207}Pb/^{206}Pb$ isotope ratio was taken as the crystallization time of ancient zircons; the $^{206}Pb/^{238}U$ age was taken as the crystallization time of young zircons.

There is no distinct criterion for calculating the age boundary separating the "young" and "old" zircons. Different authors suggest the age range from 800 to 1400 Ma (for example, Barbeau et al., 2005; Gehrels, 2012; Meinhold et al., 2008). The age of this boundary is very often determined at 1000 Ma. The crystallization age of zircons younger than 1000 Ma was calculated on the basis of the $^{206}Pb/^{238}U$ ratio; the age of zircons older than 1000 Ma was based on the $^{207}Pb/^{206}Pb$ ratio. In this work, we use the approach recommended for use in the review by Gehrels (2012).

There is no unified approach for determining the limiting discordance above which a zircon grain is excluded from further consideration. According to (Gehrels, 2012), a 30% discordance is an acceptable limit when it is necessary to save the relationships between the different-aged zircon populations; 10% discordance is acceptable only in the cases where the precise determination of the age of rocks in provenance areas is needed. It should be noted that the discordance filter certainly applies to grains whose age was calculated on the basis of the $^{207}Pb/^{206}Pb$ ratio; for younger grains whose age was calculated on the basis of the $^{206}Pb/^{238}U$ ratio, the application of the discordance filter is not so obvious. In the latter case, some authors consider that it is acceptable to use a higher discordance (for example, up to 60%; Mackey et al., 2012) or do not use it all. Accordingly, all zircons whose age is calculated on the basis of the $^{206}Pb/^{238}U$ ratio are accepted for further consideration (Beranek et al., 2006). In this work, unless otherwise stated, only grains with discordance of less than 10% were considered. The data obtained allow us to state the age of

Table. U-Pb geochronology of zircons from Samples A1, A2, A3, and A4 from the southern part of the East Anabar Basin

Number of measurement point	U, ppm	Th, ppm	Th/U	Common ^{206}Pb, %	Radiogenic ^{206}Pb, ppm	^{204}Pb-corrected isotope ratios		Error-correlation coefficient	Age, Ma		D, %
						$^{207}Pb/^{235}U$	$^{206}Pb/^{238}U$		$^{206}Pb/^{238}U$	$^{207}Pb/^{206}Pb$	
Sample A1											
A1-2.1	114	54	0.48	0.24	34	5.52 ± 1.6	0.3458 ± 1.3	0.84	1914 ± 21	1892 ± 15	–1
~~A1-6.1~~	49	1	0.03	1.89	4	0.68 ± 9.9	0.0992 ± 1.9	0.19	~~610 ± 11~~	~~178 ± 227~~	–254
~~A1-9.1~~	35	13	0.38	1.85	3	0.74 ± 11.9	0.1008 ± 2.0	0.17	~~619 ± 12~~	~~332 ± 265~~	–91
A1-13.1	40	11	0.30	0.13	19	16.50 ± 1.7	0.5623 ± 1.5	0.89	2876 ± 35	2927 ± 13	+2
~~A1-16.1~~	30	12	0.39	0.28	5	2.47 ± 3.0	0.2035 ± 1.8	0.60	~~1194 ± 19~~	~~1386 ± 46~~	+15
~~A1-20.1~~	59	27	0.47	1.91	5	0.66 ± 10.4	0.0994 ± 1.7	0.17	611 ± 10	~~111 ± 241~~	–474
A1-23.1	66	41	0.65	0.08	27	11.78 ± 1.6	0.4825 ± 1.4	0.85	2538 ± 29	2626 ± 14	+4
~~A1-27.1~~	74	32	0.45	0.06	31	14.80 ± 1.9	0.4927 ± 1.3	0.72	~~2582 ± 28~~	~~2965 ± 21~~	+16
A1-30.1	43	48	1.16	0.18	12	4.80 ± 2.9	0.3175 ± 1.6	0.54	1778 ± 24	1792 ± 45	+1
A1-34.1	107	27	0.26	0.31	33	5.81 ± 1.8	0.3569 ± 1.4	0.80	1968 ± 24	1926 ± 19	–3
A1-37.1	231	99	0.44	0.02	80	7.74 ± 1.3	0.4032 ± 1.2	0.89	2184 ± 22	2218 ± 11	+2
A1-39.1	139	45	0.34	0.08	42	5.76 ± 1.6	0.3493 ± 1.3	0.81	1931 ± 21	1949 ± 17	+1
A1-44.1	114	71	0.65	0.01	39	7.67 ± 1.4	0.4030 ± 1.3	0.91	2183 ± 24	2203 ± 10	+1
A1-48.1	77	100	1.33	0.11	34	13.29 ± 2.1	0.5086 ± 1.3	0.61	2651 ± 29	2738 ± 28	+4
A1-52.1	197	122	0.64	0.09	57	5.24 ± 1.3	0.3335 ± 1.2	0.90	1855 ± 20	1862 ± 10	0
A1-55.1	102	55	0.56	0.08	18	2.34 ± 1.8	0.2073 ± 1.3	0.76	1215 ± 15	1241 ± 23	+2
A1-57.1	122	1	0.01	0.08	36	5.58 ± 1.4	0.3439 ± 1.3	0.89	1905 ± 21	1921 ± 12	+1
A1-62.1	32	39	1.27	0.14	13	11.68 ± 1.8	0.4882 ± 1.6	0.86	2563 ± 33	2592 ± 15	+1
A1-65.1	36	30	0.85	0.73	8	3.09 ± 3.3	0.2472 ± 1.6	0.51	1424 ± 21	1438 ± 54	+1
A1-69.1	74	70	0.97	–0.07	23	6.19 ± 1.6	0.3663 ± 1.3	0.86	2012 ±23	1994 ± 14	–1
A1-72.1	116	75	0.67	0.25	48	12.00 ± 1.4	0.4865 ± 1.3	0.92	2556 ± 27	2643 ± 9	+4
A1-74.1	254	128	0.52	0.04	55	3.12 ± 1.4	0.2504 ± 1.2	0.88	1441 ± 15	1433 ± 12	–1
A1-79.1	319	45	0.14	0.06	27	0.85 ± 1.6	0.0989 ± 1.2	0.76	608 ± 7	674 ± 22	+10
A1-79.2	321	311	1.00	0.12	27	0.82 ± 2.2	0.0983 ± 1.3	0.58	605 ± 7	623 ± 39	+3
A1-79.3	525	89	0.18	0.17	41	0.74 ± 1.7	0.0908 ± 1.2	0.70	560 ± 6	560 ± 27	0
A1-83.1	53	39	0.76	0.18	22	11.56 ± 1.6	0.4929 ± 1.4	0.89	2583 ± 30	2559 ± 12	–1
A1-84.1	36	64	1.83	0.17	11	6.05 ± 2.1	0.3623 ± 1.5	0.72	1993 ± 26	1973 ± 26	–1
A1-90.1	51	46	0.95	0.46	19	9.00 ± 1.9	0.4266 ± 1.4	0.76	2290 ± 28	2380 ± 21	+4
~~A1-93.1~~	192	125	0.67	0.31	48	4.99 ± 1.5	0.2925 ± 1.2	0.83	~~1654 ± 18~~	~~2012 ± 14~~	+20
A1-97.1	16	7	0.44	0.32	5	7.23 ± 2.7	0.3930 ± 1.9	0.72	2137 ± 35	2144 ± 33	+0
A1-100.1	82	138	1.74	0.32	24	5.47 ± 1.8	0.3346 ± 1.4	0.77	1861 ± 22	1936 ± 20	+4
~~A1-105.1~~	208	129	0.64	0.92	64	7.86 ± 1.4	0.3575 ± 1.2	0.89	~~1970 ± 20~~	~~2449 ± 10~~	+23

Table. (Contd.)

Number of measurement point	U, ppm	Th, ppm	Th/U	Common ^{206}Pb, %	Radiogenic ^{206}Pb, ppm	^{204}Pb-corrected isotope ratios		Error-correlation coefficient	Age, Ma		D, %
						$^{207}Pb/^{235}U$	$^{206}Pb/^{238}U$		$^{206}Pb/^{238}U$	$^{207}Pb/^{206}Pb$	
A1-107.1	74	55	0.77	0.34	20	4.53 ± 1.9	0.3115 ± 1.4	0.74	1748 ± 21	1722 ± 23	−2
A1-110.1	72	49	0.71	0.04	44	29.47 ± 1.6	0.7157 ± 1.4	0.86	3480 ± 37	3463 ± 13	−1
A1-114.1	79	59	0.77	−0.08	24	6.05 ± 1.7	0.3525 ± 1.4	0.79	1946 ± 23	2020 ± 19	+4
~~A1-120.1~~	105	159	1.56	0.73	9	0.80 ± 4.3	0.1032 ± 1.4	0.33	~~633 ± 9~~	~~462 ± 89~~	−39
~~A1-124.1~~	123	125	1.05	0.32	11	0.79 ± 7.2	0.1008 ± 1.4	0.20	~~619 ± 9~~	~~494 ± 155~~	−27
A1-128.1	234	270	1.19	0.07	73	6.27 ± 1.3	0.3653 ± 1.2	0.93	2007 ± 21	2023 ± 9	+1
A1-132.1	74	48	0.67	0.52	23	5.91 ± 1.7	0.3577 ± 1.3	0.77	1971 ± 23	1953 ± 19	−1
A1-136.1	86	118	1.42	0.03	49	27.89 ± 1.4	0.6606 ± 1.3	0.95	3270 ± 33	3502 ± 6	+8
A1-139.1	44	26	0.60	0.35	4	0.93 ± 3.5	0.1070 ± 1.7	0.49	655 ± 10	706 ± 64	+7
A1-144.1	72	77	1.11	0.41	21	5.38 ± 1.9	0.3381 ± 1.4	0.75	1878 ± 23	1887 ± 22	+1
Sample A2											
A2-75.1	91	90	1.02	0.31	28	5.8 ± 1.7	0.354 ± 1.4	0.85	1953 ± 24	1929 ± 16	−1
~~A2-2.1~~	23	223	10.08	2.40	5	4.3 ± 5.4	0.271 ± 2.0	0.37	~~1547 ± 28~~	~~1898 ± 90~~	+21
A2-5.1	95	37	0.40	0.07	46	16.0 ± 1.5	0.565 ± 1.4	0.95	2888 ± 33	2873 ± 8	−1
A2-8.1	30	15	0.52	0.12	15	16.7 ± 2.0	0.576 ± 1.7	0.85	2931 ± 40	2905 ± 17	−1
~~A2-11.1~~	437	853	2.02	6.65	58	2.5 ± 2.6	0.154 ± 1.4	0.53	~~923 ± 12~~	~~1888 ± 39~~	+55
A2-14.1	54	50	0.96	−0.11	26	15.8 ± 1.7	0.555 ± 1.5	0.91	2847 ± 35	2877 ± 11	+1
A2-16.1	79	46	0.60	0.13	24	6.3 ± 1.9	0.362 ± 1.5	0.78	1991 ± 25	2046 ± 21	+3
A2-20.1	40	13	0.33	0.13	17	11.7 ± 1.7	0.480 ± 1.5	0.90	2526 ± 32	2628 ± 13	+5
A2-23.1	100	28	0.28	0.00	45	13.6 ± 1.5	0.523 ± 1.4	0.94	2714 ± 31	2731 ± 8	+1
A2-27.1	127	71	0.58	0.18	56	13.2 ± 1.5	0.516 ± 1.4	0.91	2682 ± 30	2707 ± 11	+1
A2-29.1	114	80	0.72	−0.02	36	6.3 ± 1.5	0.367 ± 1.4	0.91	2014 ± 24	2024 ± 11	+1
A2-32.1	52	36	0.72	0.33	24	15.5 ± 1.7	0.537 ± 1.5	0.90	2772 ± 34	2901 ± 12	+5
A2-35.1	58	83	1.48	0.09	26	13.8 ± 1.6	0.522 ± 1.5	0.92	2707 ± 33	2760 ± 11	+2
A2-38.1	60	25	0.43	0.06	19	6.5 ± 2.3	0.366 ± 1.5	0.64	2009 ± 26	2071 ± 31	+3
~~A2-41.1~~	122	120	1.02	0.45	47	11.7 ± 1.5	0.449 ± 1.4	0.92	~~2392 ± 28~~	~~2730 ± 10~~	+15
A2-44.1	67	20	0.31	0.05	30	13.5 ± 1.6	0.522 ± 1.5	0.92	2706 ± 32	2717 ± 10	0
A2-45.1	31	23	0.78	0.30	15	17.3 ± 1.8	0.578 ± 1.6	0.89	2942 ± 38	2957 ± 13	+1
A2-50.1	60	53	0.92	0.12	26	13.3 ± 1.7	0.511 ± 1.5	0.88	2659 ± 33	2736 ± 14	+3
A2-53.1	34	27	0.81	0.15	16	16.2 ± 1.8	0.560 ± 1.6	0.86	2868 ± 36	2908 ± 15	+2
A2-56.1	102	59	0.60	0.44	30	5.7 ± 1.7	0.342 ± 1.4	0.83	1898 ± 23	1953 ± 17	+3
~~A2-59.1~~	331	498	1.56	5.50	51	4.6 ± 1.8	0.181 ± 1.3	0.76	~~1071 ± 13~~	~~2691 ± 19~~	+65

Table. (Contd.)

Number of measurement point	U, ppm	Th, ppm	Th/U	Common ^{206}Pb, %	Radiogenic ^{206}Pb, ppm	^{204}Pb-corrected isotope ratios		Error-correlation coefficient	Age, Ma		D, %
						$^{207}Pb/^{235}U$	$^{206}Pb/^{238}U$		$^{206}Pb/^{238}U$	$^{207}Pb/^{206}Pb$	
A2-62.1	68	30	0.46	0.22	33	16.1 ± 1.6	0.561 ± 1.6	0.94	2871 ± 36	2887 ± 9	+1
A2-65.1	151	66	0.45	0.27	46	6.1 ± 1.6	0.353 ± 1.4	0.87	1947 ± 23	2034 ± 14	+5
A2-68.1	55	3	0.05	0.30	26	14.4 ± 1.7	0.538 ± 1.6	0.92	2773 ± 36	2783 ± 11	0
~~A2-71.1~~	111	58	0.54	0.58	47	13.6 ± 1.6	0.493 ± 1.5	0.92	~~2583 ± 32~~	~~2825 ± 10~~	+10
A2-77.1	43	14	0.33	0.16	20	15.8 ± 1.8	0.553 ± 1.6	0.88	2839 ± 36	2881 ± 14	+2
A2-80.1	41	10	0.26	0.27	20	16.3 ± 1.7	0.564 ± 1.5	0.91	2882 ± 35	2905 ± 11	+1
A2-85.1	32	47	1.49	0.36	14	13.2 ± 2.0	0.507 ± 1.8	0.89	2644 ± 39	2732 ± 15	+4
A2-88.1	53	124	2.41	0.29	24	13.7 ± 1.7	0.524 ± 1.5	0.88	2717 ± 33	2744 ± 14	+1
A2-92.1	125	145	1.20	0.33	38	5.9 ± 1.6	0.353 ± 1.4	0.88	1948 ± 23	1978 ± 13	+2
A2-94.1	49	29	0.61	0.61	15	6.2 ± 2.1	0.353 ± 1.6	0.74	1949 ± 26	2050 ± 25	+6
A2-97.1	205	69	0.35	0.12	59	5.6 ± 1.5	0.337 ± 1.3	0.88	1874 ± 22	1962 ± 13	+5
A2-100.1	67	119	1.84	0.54	19	5.1 ± 2.2	0.330 ± 1.5	0.68	1838 ± 24	1819 ± 28	–1
A2-103.1	37	14	0.38	0.48	18	16.7 ± 2.2	0.557 ± 1.7	0.77	2856 ± 39	2956 ± 22	+4
A2-106.1	70	81	1.20	0.03	32	13.8 ± 1.5	0.528 ± 1.4	0.94	2734 ± 32	2732 ± 9	0
Sample A3											
A3-2.1	88	55	0.64	0.25	28	6.4 ± 1.7	0.374 ± 1.4	0.85	2049 ± 25	2020 ± 16	–2
~~A3-6.1~~	71	85	1.24	0.14	19	5.3 ± 2.4	0.311 ± 1.5	0.64	~~1744 ± 23~~	~~2026 ± 32~~	+16
A3-11.1	78	42	0.55	0.02	24	6.3 ± 1.8	0.363 ± 1.5	0.81	1998 ± 25	2032 ± 19	+2
A3-15.1	100	64	0.67	0.14	14	1.6 ± 1.9	0.163 ± 1.4	0.78	971 ± 13	999 ± 24	+3
A3-15.2	107	64	0.62	0.21	15	1.6 ± 2.4	0.160 ± 1.6	0.66	956 ± 14	998 ± 37	+5
A3-15.3	128	82	0.66	0.16	16	1.5 ± 2.3	0.149 ± 1.6	0.70	897 ± 13	1015 ± 33	+12
A3-15.4	133	78	0.61	0.34	16	1.3 ± 2.6	0.139 ± 1.5	0.59	838 ± 12	919 ± 43	+9
A3-20.1	53	37	0.71	0.15	22	11.5 ± 1.7	0.485 ± 1.5	0.90	2551 ± 32	2574 ± 13	+1
A3-24.1	123	41	0.35	0.04	39	6.5 ± 1.5	0.372 ± 1.4	0.93	2037 ± 24	2053 ± 10	+1
A3-29.1	25	16	0.68	0.08	12	17.0 ± 1.9	0.576 ± 1.7	0.87	2931 ± 39	2940 ± 15	0
~~A3-31.1~~	366	386	1.09	0.97	58	2.9 ± 1.5	0.185 ± 1.3	0.86	~~1092 ± 13~~	~~1835 ± 14~~	+44
A3-33.1	117	172	1.52	–0.10	49	12.4 ± 2.0	0.489 ± 2.0	0.97	2567 ± 42	2684 ± 8	+5
A3-37.1	36	30	0.87	0.35	12	8.1 ± 2.1	0.410 ± 1.7	0.78	2213 ± 31	2262 ± 23	+3
~~A3-38.1~~	91	88	1.00	0.27	19	4.1 ± 1.7	0.241 ± 1.5	0.85	~~1392 ± 18~~	~~2017 ± 16~~	+34
A3-42.1	52	38	0.74	0.13	25	16.6 ± 1.6	0.568 ± 1.5	0.92	2900 ± 35	2921 ± 10	+1
A3-46.1	65	32	0.51	–0.06	27	11.9 ± 1.7	0.485 ± 1.5	0.91	2548 ± 32	2642 ± 11	+4
~~A3-47.1~~	893	1254	1.45	1.10	81	1.6 ± 1.7	0.106 ± 1.5	0.90	~~650 ± 9~~	~~1796 ± 13~~	+67

Table. (Contd.)

Number of measurement point	U, ppm	Th, ppm	Th/U	Common ^{206}Pb, %	Radiogenic ^{206}Pb, ppm	^{204}Pb-corrected isotope ratios		Error-correlation coefficient	Age, Ma		D, %
						$^{207}Pb/^{235}U$	$^{206}Pb/^{238}U$		$^{206}Pb/^{238}U$	$^{207}Pb/^{206}Pb$	
A3-50.1	57	29	0.53	0.05	28	16.4 ± 1.6	0.569 ± 1.5	0.93	2904 ± 35	2902 ± 10	0
A3-52.1	25	10	0.41	0.53	8	6.4 ± 2.8	0.383 ± 1.7	0.60	2092 ± 30	1968 ± 40	–7
A3-56.1	62	26	0.43	0.06	21	7.3 ± 1.7	0.393 ± 1.5	0.86	2137 ± 27	2171 ± 16	+2
~~A3-60.1~~	250	235	0.97	0.16	90	10.7 ± 1.4	0.417 ± 1.3	0.96	~~2247 ± 25~~	~~2707 ± 7~~	+20
A3-61.1	6	12	2.08	0.78	2	5.6 ± 9.1	0.345 ± 3.0	0.34	1911 ± 50	1917 ± 153	0
A3-65.1	95	44	0.48	0.14	26	5.0 ± 1.6	0.318 ± 1.4	0.88	1780 ± 22	1876 ± 14	+6
A3-69.1	163	87	0.55	0.04	75	14.7 ± 1.4	0.535 ± 1.3	0.97	2761 ± 30	2827 ± 5	+3
A3-73.1	114	176	1.59	0.05	35	5.9 ± 1.5	0.359 ± 1.4	0.91	1978 ± 24	1953 ± 11	–2
A3-78.1	56	68	1.26	0.07	17	6.1 ± 1.8	0.362 ± 1.5	0.85	1993 ± 26	1977 ± 17	–1
~~A3-82.1~~	63	56	0.92	0.70	21	8.0 ± 2.1	0.389 ± 1.6	0.75	~~2119 ± 29~~	~~2331 ± 24~~	+11
A3-87.1	115	59	0.53	0.08	54	15.4 ± 1.5	0.549 ± 1.4	0.95	2820 ± 32	2852 ± 8	+1
A3-92.1	75	102	1.40	0.12	28	9.7 ± 1.7	0.432 ± 1.4	0.85	2315 ± 28	2487 ± 15	+8
~~A3-96.1~~	67	153	2.36	0.27	8	1.5 ± 2.9	0.147 ± 1.6	0.56	~~882 ± 13~~	~~979 ± 49~~	+11
A3-99.1	159	103	0.67	0.04	47	5.5 ± 1.5	0.342 ± 1.4	0.92	1894 ± 22	1921 ± 10	+2
A3-102.1	49	31	0.65	0.05	22	13.5 ± 1.8	0.518 ± 1.5	0.84	2691 ± 33	2728 ± 16	+2
A3-105.1	57	21	0.38	0.20	28	16.9 ± 1.5	0.569 ± 1.4	0.94	2903 ± 33	2944 ± 9	+2
~~A3-110.1~~	708	201	0.29	0.01	258	10.5 ± 1.3	0.424 ± 1.3	0.99	~~2280 ± 25~~	~~2655 ± 3~~	+17
A3-114.1	97	48	0.51	–0.10	30	6.3 ± 1.6	0.367 ± 1.4	0.85	2013 ± 24	2026 ± 15	+1
A3-116.1	137	42	0.32	0.11	46	7.2 ± 1.4	0.390 ± 1.3	0.94	2124 ± 24	2149 ± 9	+1
A3-121.1	16	11	0.69	–0.55	5	6.3 ± 2.7	0.357 ± 1.9	0.69	1969 ± 32	2075 ± 35	+6
A3-123.1	23	25	1.11	0.27	9	10.3 ± 2.1	0.454 ± 1.8	0.84	2412 ± 35	2510 ± 19	+5
A3-125.1	41	41	1.03	0.08	22	22.9 ± 1.7	0.634 ± 1.5	0.90	3164 ± 38	3258 ± 11	+4
~~A3-128.1~~	8	11	1.43	3.10	2	4.9 ± 5.6	0.340 ± 2.5	0.45	~~1887 ± 41~~	~~1716 ± 93~~	–12
A3-131.1	30	91	3.14	0.23	9	5.7 ± 2.2	0.340 ± 1.7	0.78	1888 ± 28	1989 ± 24	+6
Sample A4											
A4-1.1	114	85	0.77	0.08	35	5.9 ± 1.5	0.356 ± 1.4	0.91	1964 ± 23	1971 ± 11	0
A4-4.1	50	17	0.36	0.17	16	6.4 ± 1.8	0.378 ± 1.5	0.86	2065 ± 27	2010 ± 16	–3
A4-7.1	145	103	0.73	0.08	43	5.7 ± 1.5	0.349 ± 1.3	0.92	1931 ± 22	1933 ± 10	0
A4-10.1	68	45	0.69	0.23	20	5.7 ± 1.7	0.346 ± 1.5	0.87	1916 ± 24	1943 ± 15	+2
~~A4-15.1~~	20	39	1.96	1.57	5	5.0 ± 3.6	0.300 ± 1.8	0.51	~~1691 ± 27~~	~~1960 ± 55~~	+16
A4-16.1	126	141	1.16	0.50	37	5.6 ± 1.7	0.343 ± 1.4	0.82	1899 ± 23	1920 ± 18	+1
A4-19.1	110	53	0.50	0.14	32	5.5 ± 1.5	0.342 ± 1.4	0.91	1896 ± 23	1907 ± 12	+1

Table. (Contd.)

Number of measurement point	U, ppm	Th, ppm	Th/U	Common ^{206}Pb, %	Radiogenic ^{206}Pb, ppm	^{204}Pb-corrected isotope ratios		Error-correlation coefficient	Age, Ma		D, %
						$^{207}Pb/^{235}U$	$^{206}Pb/^{238}U$		$^{206}Pb/^{238}U$	$^{207}Pb/^{206}Pb$	
A4-21.1	150	80	0.55	0.24	44	5.7 ± 1.6	0.345 ± 1.4	0.87	1912 ± 23	1948 ± 14	+2
A4-25.1	186	81	0.45	0.03	55	5.6 ± 1.5	0.342 ± 1.4	0.89	1898 ± 22	1949 ± 12	+3
A4-28.1	45	87	1.98	0.49	14	5.9 ± 2.0	0.357 ± 1.6	0.79	1968 ± 27	1957 ± 22	−1
A4-32.1	129	212	1.71	0.59	39	5.8 ± 1.7	0.350 ± 1.4	0.84	1936 ± 23	1959 ± 16	+1
A4-31.1	42	16	0.40	−0.05	15	8.9 ± 1.8	0.416 ± 1.5	0.85	2243 ± 29	2405 ± 16	+8
A4-34.1	113	144	1.32	0.23	48	12.8 ± 1.5	0.496 ± 1.4	0.92	2597 ± 30	2711 ± 10	+5
A4-37.1	52	20	0.40	0.09	25	16.4 ± 1.7	0.559 ± 1.5	0.86	2865 ± 35	2929 ± 14	+3
A4-40.1	87	41	0.49	0.10	27	6.0 ± 1.7	0.357 ± 1.5	0.89	1966 ± 26	1973 ± 14	0
A4-43.1	61	33	0.56	0.31	20	6.3 ± 1.8	0.374 ± 1.5	0.84	2048 ± 27	1996 ± 18	−3
A4-46.1	57	50	0.91	0.66	26	15.4 ± 1.9	0.530 ± 1.6	0.84	2742 ± 36	2912 ± 17	+7
A4-49.1	83	203	2.52	0.40	36	12.4 ± 1.6	0.496 ± 1.5	0.90	2599 ± 31	2666 ± 12	+3
A4-52.1	21	8	0.41	1.14	10	16.3 ± 2.3	0.564 ± 1.8	0.80	2884 ± 42	2902 ± 22	+1
A4-55.1	71	32	0.47	−0.10	21	5.8 ± 1.8	0.349 ± 1.5	0.85	1928 ± 25	1969 ± 17	+2
A4-58.1	176	102	0.60	0.02	54	5.8 ± 1.5	0.356 ± 1.3	0.87	1961 ± 23	1940 ± 14	−1
A4-61.1	159	67	0.44	0.23	46	5.6 ± 1.9	0.336 ± 1.4	0.75	1870 ± 23	1965 ± 22	+6
A4-64.1	39	46	1.21	0.31	12	5.6 ± 2.0	0.349 ± 1.7	0.83	1932 ± 28	1913 ± 20	−1
A4-67.1	60	57	0.98	0.13	25	12.3 ± 1.7	0.490 ± 1.5	0.90	2569 ± 33	2673 ± 12	+5
A4-70.1	12	0	0.01	0.80	4	5.7 ± 3.2	0.349 ± 2.1	0.67	1929 ± 36	1934 ± 42	0
A4-73.1	69	65	0.98	−0.14	21	5.9 ± 1.8	0.351 ± 1.5	0.84	1941 ± 26	1986 ± 18	+3
~~A4-76.1~~	425	796	1.93	3.02	53	2.2 ± 2.0	0.144 ± 1.4	0.66	~~869 ± 11~~	~~1808 ± 28~~	+55
A4-79.1	126	92	0.76	0.12	40	6.4 ± 1.6	0.365 ± 1.4	0.90	2006 ± 24	2047 ± 12	+2
A4-81.1	119	89	0.78	0.04	53	13.4 ± 1.4	0.516 ± 1.4	0.95	2683 ± 30	2729 ± 7	+2
A4-86.1	153	99	0.67	0.22	46	5.8 ± 1.6	0.348 ± 1.4	0.88	1925 ± 23	1962 ± 14	+2
A4-88.1	51	131	2.64	0.44	16	6.1 ± 2.2	0.365 ± 1.5	0.69	2005 ± 27	1970 ± 29	−2
A4-91.1	159	112	0.73	0.05	48	5.8 ± 1.5	0.349 ± 1.4	0.92	1932 ± 23	1967 ± 11	+2
A4-94.1	54	18	0.34	0.46	25	15.6 ± 1.6	0.546 ± 1.5	0.91	2809 ± 34	2886 ± 11	+3
A4-97.1	78	59	0.78	0.64	22	5.4 ± 2.2	0.334 ± 1.5	0.67	1857 ± 24	1919 ± 30	+4
A4-100.1	143	88	0.64	0.10	84	28.2 ± 1.6	0.687 ± 1.4	0.89	3370 ± 37	3459 ± 11	+3
A4-104.1	40	22	0.56	0.22	20	19.0 ± 2.5	0.581 ± 2.1	0.86	2951 ± 50	3106 ± 20	+6
~~A4-107.1~~	118	97	0.85	0.25	33	5.7 ± 1.6	0.325 ± 1.4	0.87	~~1812 ± 22~~	~~2076 ± 14~~	+15
A4-110.1	174	163	0.97	0.13	63	9.2 ± 1.5	0.422 ± 1.4	0.93	2269 ± 26	2439 ± 9	+8

The data errors are at 1σ. Discordance index (D) is calculated as 100 × (1 − (age $^{206}Pb/^{238}U$)/(age $^{207}Pb/^{206}Pb$)). Ages with discordance greater than 10% are struck through. In grain A1-79, dating was performed at three measurement points (A1-79.1, A1-79.2, and A1-79.3); in grain A3-15, at four measurement points (A3-15.1, A3-15.2, A3-15.3, and A3-15.4).

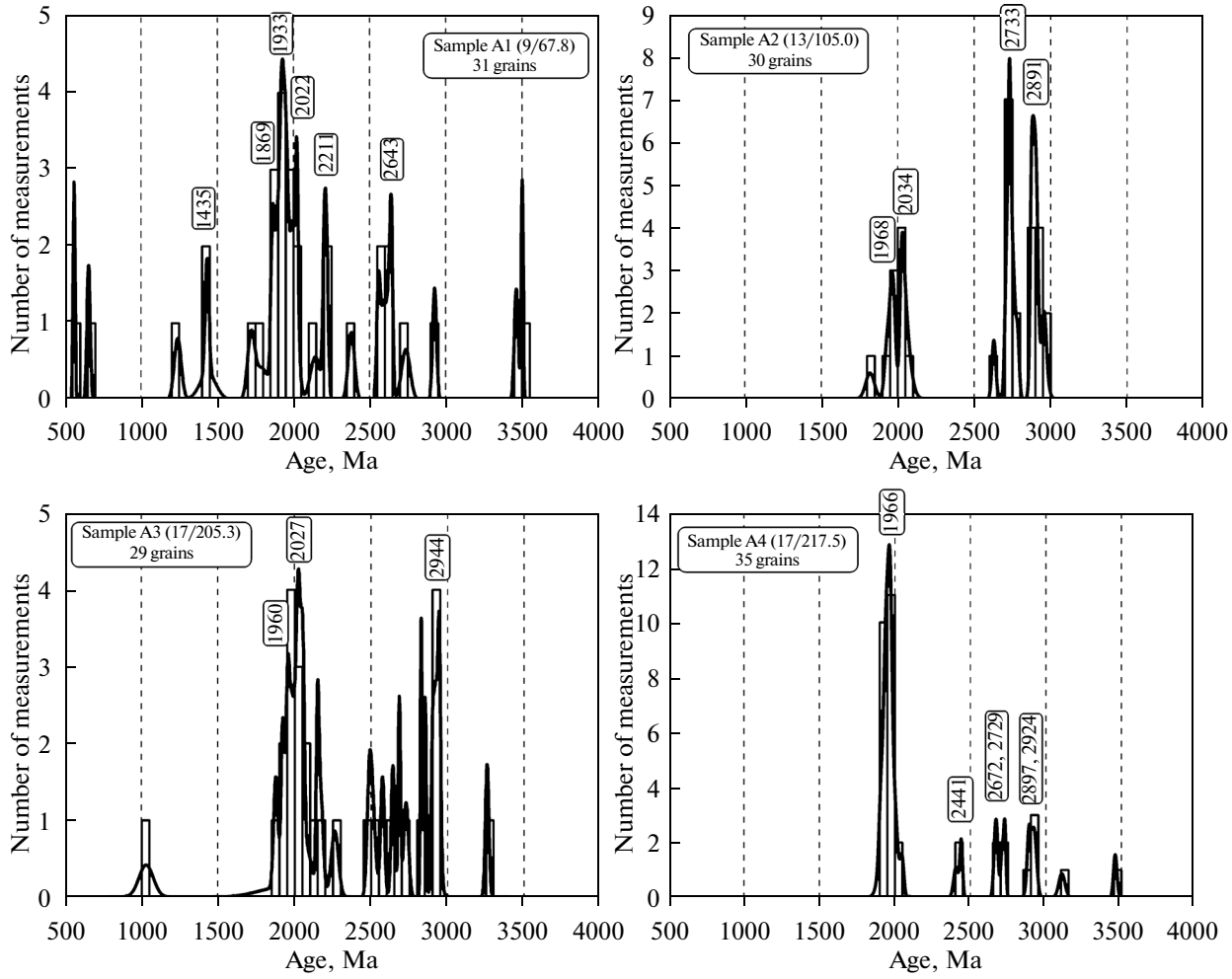

Fig. 4. Age distribution plots (histograms and probability curves) for detrital zircons from samples of sandstones sampled in the southern part of the East Anabar Basin.

rocks in a provenance area with a high confidence level. Of the 151 studied grains, only 125 grains meet these criteria. The age datings of these grains are considered below. To clarify the age of two samples (A1-79 and A3-15), measurements were made at several points, so that there were 156 measurement points in total.

RESULTS OF ISOTOPIC INVESTIGATION

Most of the detrital zircons from sandstones of the southern part of the East Anabar Basin are subisometric and isometric in shape and about 100 μm in size (Fig. 3). In fact, these grains preserved crystallographic faceting and bear the signs of substantial physical abrasion. Some grains are characterized by a distinct internal zoning, while others have metamorphic rims or homogeneous internal structures.

The most of the zircon grains contain low and moderate uranium contents. A U content of more 300 ppm was measured only in 7 of 151 grains with a maximum content of 893 ppm. Abnormally low uranium contents (less than 20 ppm) at low thorium contents were measured in five zircon grains, three of them in Sample A3. The Th/U ratio varies in a wide range from 0.01 to 10.08. There is no correlation between the uranium content and the Th/U ratio.

Results of U-Pb dating of detrital zircons are shown on age distribution plots (Fig. 4).

In Sample A1, collected in the top of strata 4 (Fig. 2), the ages of 9 of 36 zircon grains are in the range of 1950–2050 Ma, and the ages of 8 of 36 zircon grains are of Archean age, including the most ancient zircon grain with $^{207}Pb/^{206}Pb$ age of 3502 ± 6 Ma (Fig. 4). Three detrital grains have Riphean age of 1241 ± 23, 1433 ± 12, and 1438 ± 54 Ma. The youngest zircon grain (A1-79) was dated at three points. Although the lower intersection age is characterized by a large error (562 ± 41 Ma, Fig. 5), it is very close to the youngest of the three age datings of grain A1-79—concordant age of 560 ± 6 Ma (A1-79.3, table). At the same time, seven age datings, two of which for grain A1-79 (points A1-79.1 and A1-79.2) and the remain-

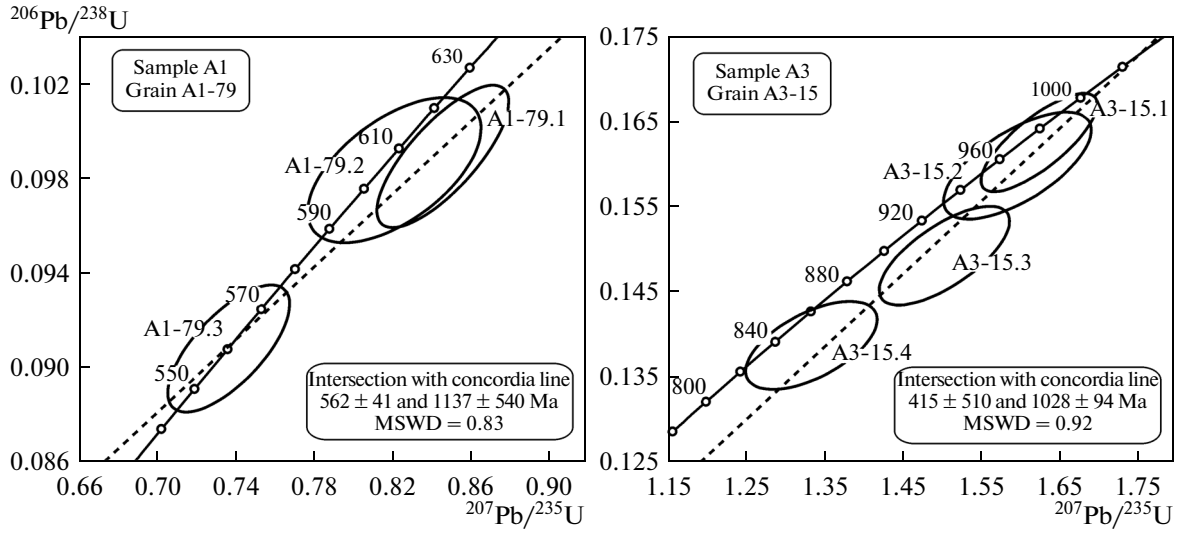

Fig. 5. Concordia diagrams for the youngest detrital zircons from Samples A1 and A3. Data error ellipses are 2σ. Numbers of measurement points on plots correspond to those in the table.

ing five grains for grains with high discordance level, yield a concordant age of 614 ± 11 Ma (Fig. 6), which allows us to relate these grains, including A1-79, to a single magmatic event in a provenance area. This contradiction does not allow us to make an unambiguous conclusion which age, 560 ± 6 or 614 ± 11 Ma, should be considered as the age of the youngest detrital zircons in Sample A1.

In Sample A2, collected in the upper part of stratum 2, 20 of 30 zircon grains are of Archean age with distinct peaks of around 2700–2750 and 2850–2950 Ma (Fig. 4). The age of most of the other zircons lies in the interval of 1950–2050 Ma.

In Sample A3, collected at the base of stratum 2, 12 of 30 zircon grains are of Archean age with distinct peak values of 2900–2950 Ma (Fig. 4). Most of the grains (16 of 30) have Early Proterozoic age. This fraction of zircon grains is dominated by detrital grains with age interval of 1900–2060 Ma. The age of the youngest grain (A3-15), dated at four points and calculated on the upper intersection, is 1028 ± 94 Ma (Fig. 5).

In Sample A4, collected at the base of the section, 23 of 35 zircon grains lie in the age interval of 1900–2050 Ma and only 10 zircon grains are of Archean age (Fig. 4).

All age distribution plots of detrital zircons from different samples (Fig. 4) are characterized by a large degree of similarity. According to this, we can suggest that detrital zircons originated from the same source areas. Most of the zircon grains are related to erosion of rocks with age of 1900–2050 Ma; a smaller proportion of zircon grains have Archean age, which is evidence of the Early Proterozoic intensive reworking of the Archean basement at a great distance from the sedimentation area of Archean rocks. Late Archean zircons with two peaks of 2700–2750 and 2850–2950 Ma dominate.

DISCUSSION OF RESULTS

The section of Riphean–Vendian deposits in the southern part of the East Anabar Basin, as well as in the entire basin, has a two-unit terrigenous-carbonate structure (Fig. 7). Compositionally and structurally, the lower terrigenous unit of the section, consisting mainly of sandstones and conglomerates, is similar to the Mukun Group, except for the fact that the deposits of the Mukun Group are of fluvial origin (*Opornyi...*, 1970; *Gosudarstvennaya...,* 1983; Petrov, 2011), whereas the

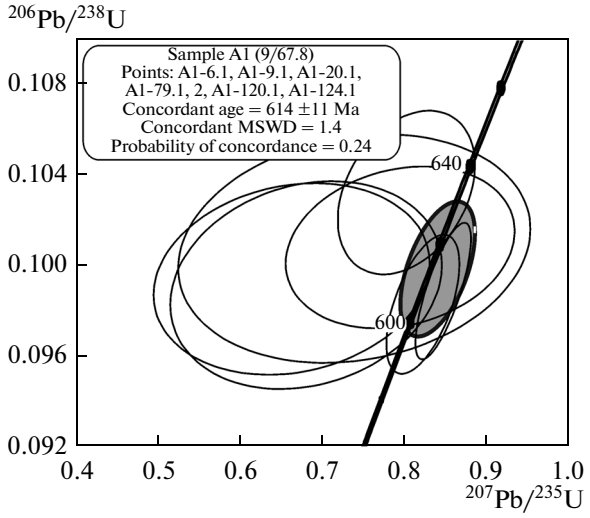

Fig. 6. Concordia diagrams for zircon grains of Al-6, Al-9, Al-20, Al-120, A1-124, and A1-79 (measurements A1-79.1 and A1-79.2).

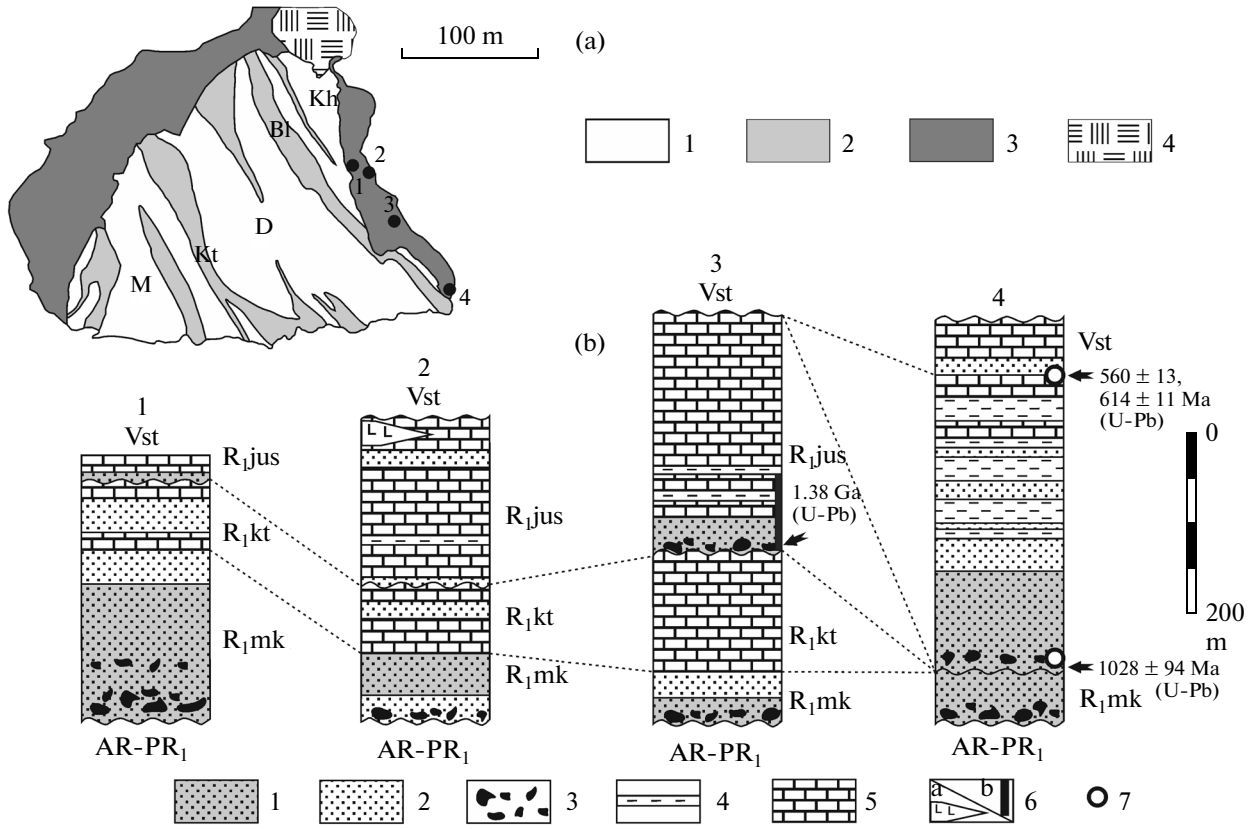

Fig. 7. Riphean deposits of the southeastern part of the Anabar Shield. (a) Geological scheme of the Anabar Shield, after (*Gosudarstvennaya...*, 1983; Rozen, 1995), simplified: (1) Archean–Proterozoic terrains and belts (M—Magan, D—Daldyn, Kh—Khapchan); (2) Early Proterozoic mélange zones (Kt—Kotuikan-Monkhool, Bl—Billyakh); (3) Riphean sedimentary cover; (4) Popigai astrobleme. Black circles with figures show location of sections in Fig. 7b. (b) Correlation scheme of Upper Precambrian reference sections in the northern, central (*Gosudarstvennaya...*, 1969, 1972, 1987), and southern parts of the East Anabar Basin: (1) subarkoses; (2) quartz sandstones; (3) conglomerates; (4) claystones nd siltstones; (5) dolomites; (6) basic volcanites: (a) lavas, tuffs; (b) dikes and their ages (Ernst et al., 2000); (7) sites of Samples A1 and A3; age datings of youngest zircons from these samples. Abbreviations: mk—Mukun Group; kt—Kotuikan Formation of the Billyakh Group; jus—Yusmastakh Formation of the Billyakh Group; st—Starorechenskaya Formation.

southern part of the basin was deposited in a fluvial and coastal marine environment.

The correlation of the upper terrigenous-carbonate stratum with the facially variably Billyakh Group is more complex. In the central part of the East Anabar Basin (Fig. 7), the Billyakh Group is mainly composed of sandy and algal dolomites with interlayers and lenses of sandstones and conglomerates (*Gosudarstvennaya...*, 1969, 1972, 1987). The sequence of terrigenous-carbonate deposits in the southern part of the basin is dominated by interbedded siltstones and mudstones, which is more typical of the Ust-Il'inskaya Formation (the base of the Billyakh Group) of the West Anabar Basin. The latter is also composed mainly of siltstones and mudstones with interbedded glauconite sandstones and dolomites (*Opornyi...*, 1970; Gorokhov et al., 1991; Veselovskii et al., 2009).

However, the U-Pb dating of detrital zircons showed that the stratigraphy of Riphean deposits varies in different parts of the East Anabar Basin (Fig. 7). The age of grain A3-15 (Fig. 5) indicates that the age of host sandstones of stratum 2 must be younger than about 1030 Ma. This means that these deposits and the overlying strata have Late Riphean age and cannot be related to the Mukun Group. The terrigenous stratum demonstrates numerous erosion zones, including one in the lower part of the section, which apparently fixes a significant stratigraphic gap, separating Upper Riphean and Lower Riphean (relics of the Mukun Group) sandstones. Although the entire northeastern part of the basin has Early Riphean age, the thickness of Early Riphean sediments is reduced to 70 m in the south (Fig. 7).

The terrigenous-carbonate strata located stratigraphically above the relics of the Mukun Group also has Late Riphean age and cannot be correlated with the Billyakh Group. There are no age analogs of this stratum in the central and northern parts of the East Anabar Basin or in the West Anabar Basin (Fig. 7).

Some part of the mudstone-dolomitic stratum previously assigned to the Billyakh Group lies below analogs of Vendian stratum of the Starorechenskaya For-

mation and, accordingly, must be older than the latter. At the same time, it is characterized by a large number of Vendian zircon grains, indicating that the host rocks should also be attributed to the Vendian.

Thus, the structure of the southern part of the East Anabar Basin is apparently related to the transgressive overlap of Upper Vendian–Lower Riphean rocks on eroded deposits of the Mukun and Billyakh groups (Fig. 7).

Along with the possibility to determine the age of host deposits, the U-Pb dating of detrital zircons is of importance for reconstruction of provenance areas of sedimentary material. Here, for the correct interpretation, it is necessary to take into account that in each sample only 29–35 grains were analyzed. This provides information on approximately 90% of the total population of zircons with a probability of 95% (McLennan et al., 2003), which is sufficient for identification of major provenance areas. Accordingly, one can make preliminary conclusions, but owing to a lack of information on approximately 10% of the population of zircons, secondary sources of sedimentary material can be missed.

The predominance of detrital zircons with the Th/U ratio greater than 0.5 is evidence that mainly igneous rocks were eroded (Hoskin and Schaltegger, 2003). At the same time, the presence of five grains with abnormally low contents of uranium and thorium (less than 20 ppm) indicates an occurrence of an unusual provenance area, which can be identified by studying the geochemical parameters in the future. The age of these grains is in the range of about 1930–2150 Ma.

As seen in the plots in Figs. 4, the formation of Riphean sandstones in the southern part of the East Anabar Basin is a consequence of the erosion of predominantly Archean crust, intensively reworked at about 1950–2050 Ma. In comparison with results of studying sandstones from the base of the Riphean sequence northward of the West Anabar Basin (Khudoley et al., 2007) and age datings of zircons from Sample A4, Samples A3 and A2 show a significant increase in the number of Archean zircon grains. This is evidence that a considerable proportion of Late Proterozoic rocks were eroded.

The rocks of the Billyakh and neighboring mélange zones were probably a source of zircons with ages of 1950–2050 Ma; the peak value of 2850–2950 Ma is probably related to the erosion of granulites of the Magan and Daldyn terranes (Rosen et al., 2000; Molchanov et al., 2011; Smelov et al., 2012; Gusev et al., 2013; Smelov and Timofeev, 2007).

On the basis of Nd isotopic data, it was earlier established that conglomerate-sandstone and sandy-siltstone strata of the southern part of the East Anabar Basin have Archean Nd model ages, similar to those of granulito-gneisses of the Magan and Daldyn terranes, as well as anorthosites of the Kotuikan zone (Kuptsova et al., 2011; Molchanov et al., 2011; Gusev et al., 2013). The upper stratum, containing Vendian detrital zircons, has the same Nd isotopic characteristics as granulites of the Birektin terrane and products of their erosion—garnet paragneisses of the Khapchan belt (Kuptsova et al., 2011). Measurements of cross-bedding indicate the eastern orientation of paleoflows, which also confirms erosional processes in ancient crystal blocks of the Anabar Uplift.

Age datings in a range of about 2700–2750 Ma are not common for the Anabar Uplift.

The origin of the Riphean and Vendian detrital zircon grains remains unclear. Igneous rocks of this age within the Anabar Shield and the central part of the Siberian platform are not found. The eastern orientation of paleoflows contradicts the idea of the supply of zircons from the eastern margin of the Siberian Platform. The most probable provenance area could be the Taimyr Orogen, where metarhyolites (627 ± 7 Ma) and metamorphic events (625–575 Ma), close in age, were established (Vernikovsky et al., 1997; Vernikovsky et al., 2004). The igneous complexes similar in age are known in the southern and southwestern folded framing of the Siberian Platform (Vernikovsky et al., 2004; Vernikovsky and Vernikovskaya, 2006; Rytsk et al., 2007), but in the Late Vendian, the greater part of the Siberian platform was flooded with water and the transfer of the detrital material through a sea basin over a considerable distance seems unlikely.

In order to explain the occurrence of erosion products of Riphean and Vendian igneous rocks in the central part of the Siberian Platform, additional studies need to be performed.

CONCLUSIONS

As a result of this work the following conclusions were made:

(1) The Riphean section in the southeastern margin of the Anabar Shield comprises both the Lower and Upper Riphean strata. The latter have no analogs in the Riphean sequences located northward. The most upper part of the section, traditionally regarded as Riphean, has Vendian age.

(2) The provenance area was represented by magmatic or metamorphic rocks with abnormally low U and Th concentrations (less than 20 ppm).

(3) In general, the age of detrital zircons in samples from the Riphean section corresponds to the age of rocks exposed within the Anabar Shield. The Early Proterozoic detrital zircons dominate in the sample from the lower part of the Riphean section. Higher in the section, the number of zircon grains of Archean age increases markedly, indicating that a significant part of Late Proterozoic rocks were eroded.

(4) The Vendian sandstones contain material that originated from a provenance area with age of 614 ± 11 Ma, most probably, from the Taimyr Orogen.

ACKNOWLEDGMENTS

We are grateful to A.V. Soloviev and E.V. Bibikova for constructive reviews.

This work was supported by Cameco (Canada), R&D project no. 3.39.139.2014 (St. Petersburg State University), and the Russian Foundation for Basic Research (project no. 13-05-00943).

Reviewers A.V. Soloviev and E.V. Bibikova

REFERENCES

Barbeau, Jr., D.L., Ducea, M.N., Gehrels, G.E., et al., U-Pb detrital-zircon geochronology of Northern Salinian basement and cover rocks, *GSA Bull.*, 2005, vol. 117, nos. 3/4, pp. 466–481.

Beranek, L.P., Link, P.K., and Fanning, C.M., Miocene to Holocene landscape evolution of the Western Snake River plain region, Idaho: using the SHRIMP detrital zircon provenance record to track eastward migration of the Yellowstone hotspot, *GSA Bull.*, 2006, vol. 118, nos. 9/10, pp. 1027–1050.

Ernst, R.E., Buchan, K.L., Hamilton, M.A., et al., Integrated paleomagnetism and U-Pb geochronology of mafic dikes of the Eastern Anabar Shield region, Siberia: implications for Mesoproterozoic paleolatitude of Siberia and comparison with Laurentia, *J. Geol.*, 2000, vol. 108, no. 3, pp. 381–401.

Gehrels, G., Detrital zircon U-Pb geochronology: current methods and new opportunities, in *Tectonics of Sedimentary Basins: Recent Advances. Ch. 2*, Blackwell, 2012, pp. 47–62.

Gladkochub, D.P., Stanevich, A.M., Travin, A.V., et al., The Mesoproterozoic Udzha paleorift (Northern Siberian Craton): new data on age of basites, stratigraphy, and microphytology, *Dokl. Earth Sci.*, 2009, vol. 425, no. 5, pp. 371–377.

Gorokhov, I.M., Semikhatov, M.A., Drubetskoi, E.R., et al., Rb-Sr and K-Ar age of sedimentary geochronometers from the Lower Riphean of the Anabar Massif, *Izv. Akad. Nauk SSSR, Ser. Geol.*, 1991, no. 7, pp. 17–32.

Gorokhov, I.M., Semikhatov, M.A., Mel'nikov, N.N., et al., Rb-Sr geochronology of Middle Riphean shales, the Yusmastakh Formation of the Anabar Massif, Northern Siberia, *Stratigr. Geol. Correl.*, 2001, vol. 9, no. 3, pp. 213–231.

Gosudarstvennaya geologicheskaya karta SSSR. Masshtab 1 : 200000. Listy R-49-XXIII, XXIV. Ob"yasnitel'naya zapiska (The 1 : 200000 State Geological Map of the USSR. Sheets: R-49-XXIII, XXIV. Explanatory Note), Moscow: Nedra, 1969 [in Russian].

Gosudarstvennaya geologicheskaya karta SSSR. Masshtab 1 : 200000. Listy R-49-XV, XVI. Ob"yasnitel'naya zapiska (The 1 : 200000 State Geological Map of the USSR. Sheets:-49-XV, XVI. Explanatory Note), Moscow: Nedra, 1972 [in Russian].

Gosudarstvennaya geologicheskaya karta SSSR. Masshtab 1 : 1000000. List R-48-(50)-Olenek (The 1 : 1000000 State Geological Map of the USSR. Sheet R-48-(50)-Olenek), Markov, F.G., Ed., Leningrad: VSEGEI, 1983 [in Russian].

Gosudarstvennaya geologicheskaya karta SSSR. Masshtab 1 : 200000. Listy R-48-XI, XII; R-49-I, II; R-49-VII, VIII; R-49-XIII, XIV. Ob"yasnitel'naya zapiska (The 1 : 200000 State Geological Map of the USSR. Sheets: R-48-XI; R-49-I, II; R-49-VII; R-49-XIII, XIV. Explanatory Note), Moscow: Nedra, 1987 [in Russian].

Gusev, N.I., Rudenko, V.E., Berezhnaya, N.G., et al., Isotope-geochemical features and age (SHRIMP II) of metamorphic and magmatic rocks in the Kotuikan-Monkholin zone of the Anabar Shield, *Regional. Geol. Metallog.*, 2013, no. 54, pp. 45–59.

Hoskin, P.W.O. and Schaltegger, U., The composition of zircon and igneous and metamorphic petrogenesis, in *Zircon*, Hanchar, J.M. and Hoskin, P.W.O., Eds., *Rev. Mineral. Geochem.*, 2003, vol. 53, pp. 27–62.

Khudoley, A.K., Molchanov, A.V., Okrugin, A.V., et al., Evolution of the North Siberian Platform basement as evidenced from U-Pb data from detrital zircons in sandstones of the Mukun Group, Anabar Shield, in *Fundamental'nye problemy geotektoniki. Mat. XL Tekton. Soveshch.* (Proc. XL Tecton. Meet. "Fundamental Problems of Geotectonics"), Moscow: GEOS, 2007, vol. 2, pp. 333–335.

Khudoley, A.K., Chamberlain, K.R., Schmitt, A.K., et al., New baddeleyite U-Pb data for mafic rocks of Taimyr, northern and southeastern parts of Siberia and their significance for studying the tectonics and stratigraphy of the Siberian Region, in *Izotopnye sistemy i vremya geologicheskikh protsessov. Mat. IV Ross. konf. po izotopnoi geologii. T. 2* (Proc. IV Russ. Conf. on Isotope Geology "Isotopic Systems and Time of Geological Processes". Vol. II), St. Petersburg: IP Katalkina, 2009, pp. 243–245.

Kuptsova, A.V., Khudoley, A.K., and Molchanov, A.V., Lithogeochemistry of Meso- and Neoproterozoic terrigenous rocks of the southeast Anabar Basin: evolution of the composition of source rocks and epigenetic alterations, *Vestn. St. Petersburg. Univ., Ser. 7.*, 2011, no. 1, pp. 17–31.

Ludwig, K.R., SQUID 1.02, A User's Manual, *Berkeley Geochronol. Center Spec. Publ.*, 2000, no. 2.

Ludwig, K.R., User's Manual for Isoplot 3.00: A Geochronological Toolkit for Microsoft Excel, *Berkeley Geochronol. Center Spec. Publ.*, 2003, no. 4.

Mackey, G.N., Horton, B.K., and Milliken, K.L., Provenance of the Paleocene–Eocene Wilcox Group, Western Gulf of Mexico Basin: evidence for integrated drainage of the Southern Laramide Rocky Mountains and Cordilleran Arc, *GSA Bull.,* 2012, vol. 124, nos. 5/6, pp. 1007–1024.

McLennan, S.M., Bock, B., Hemming, S.R., et al., The roles of provenance and sedimentary processes in the geochemistry of sedimentary rocks, in *Geochemistry of Sediments and Sedimentary Rocks: Evolutionary Considerations to Mineral Deposit-Forming Environments*, Lentz, D.R., Ed., *Geol. Assoc. Can. Geotext.*, 2003, vol. 4, pp. 7–38.

Meinhold, G., Reischmann, T., Kostopoulos, D., et al., Provenance of sediments during subduction of Palaeotethys: detrital zircon ages and olistolith analysis in Palaeozoic sediments from Chios Island, Greece, *Palaeogeogr. Palaeoclimat. Palaeoecol.*, 2008, vol. 263, pp. 71–91.

Molchanov, A.V., Efimov, S.A., and Klyuev, N.K., Metallogenic zoning and prognosis evaluation of uranium in the Anabar Shield, *Prirodn. Resursy Taimyra*, 2003, no. 1, pp. 34–54.

Molchanov, A.V., Metallogeny of uranium in the Aldan and Anabar Shields, *Extended Abstract of Doctoral (Geol.-Mineral.) Dissertation*, St. Petersburg: VSEGEI, 2004.

Molchanov, A.V., Knyazev, V.Yu., and Khudoley, A.K., Tectonic-fluid zones of the Anabar Shield and their ore potential, *Regional. Geol. Metallogen.*, 2011, no. 47, pp. 96–106.

Opornyi razrez verkhnedokembriiskikh otlozhenii zapadnogo sklona Anabarskogo podnyatiya (The Reference Section of Upper Precambrian Deposits on the Western Slope of the Anabar Uplift), Tkachenko, B.V., Ed., Leningrad: NIIGA, 1970 [in Russian].

Petrov, P.Yu., Facies characteristics and terrigenous sedimentation features of the Lower Riphean Mukun Group (Anabar Uplift, Siberia), *Lithol. Mineral. Resour.*, 2011, vol. 46, no. 2, pp. 165–185.

Rozen, O.M., Metamorphic effects of tectonic movements at the lower crust level: zones of Proterozoic collision and terranes of the Anabar Shield, *Geotectonics*, 1995, no. 2, pp. 91–101.

Rozen, O.M., Zhuravlev, D.Z., Sukhanov, M.K., et al., Early Proterozoic terranes, collision zones, and associated anorthosites in the northeast of the Siberian Craton: Isotope geochemistry and age characteristics, *Russ. Geol. Geophys.*, 2000, vol. 41, no. 2, pp. 163–179.

Rozen, O.M., Manakov, A.V., and Zinchuk, N.N., *Sibirskii kraton: formirovanie, almazonosnost'* (The Siberian Craton: Evolution and Diamond Potential), Moscow: Nauchn. Mir, 2006 [in Russian].

Rytsk, E.Yu., Kovach, V.P., Kovalenko, V.I., and Yarmolyuk, V.V., Structure and evolution of the continental crust in the Baikal Fold Region, *Geotectonics*, 2007, vol. 41, no. 6, pp. 460–464.

Semikhatov, M.A. and Serebryakov, S.N., *Sibirskii gipostratotip rifeya* (The Siberian Hypostratotype of the Riphean), Moscow: Nauka, 1983 [in Russian].

Sergeev, V.N., Silicified Riphean microfossils of the Anabar Uplift, *Stratigr. Geol. Correl.*, 1993, vol. 1, no. 3, pp. 264–278.

Sergeev, V.N., Vorob'eva, N.G., and Petrov, P.Yu., New data on the location of Riphean microbiota of the Bilyakh Group in the Northern Anabar Region (Fomich River basin): implication for the Riphean biostratigraphy of the Siberian Craton, *Stratigr. Geol. Correl.*, 2007, vol. 15, no. 1, pp. 3–12.

Smelov, A.P. and Timofeev, V.F., The age of the North Asian cratonic basement: an overview, *Gondwana Res.*, 2007, vol. 12, pp. 279–288.

Smelov, A.P., Kotov, A.B., Sal'nikova, E.B., et al., Age and duration of the formation of the Billyakh tectonic melange zone, Anabar Shield, *Petrology*, 2012, vol. 20, no. 3, pp. 286–300.

Stern, R.A., The GSC Sensitive High Resolution Ion Microprobe (SHRIMP): analytical techniques of zircon U-Th-Pb age determinations and performance evaluation, in *Age and Isotopic Studies*, 1997, Rep. 10, Pap. 97-1F, pp. 1–31.

Stern, R.A. and Amelin, Y., Assessment of errors in SIMS zircon U-Pb geochronology using a natural zircon standard and NIST SRM 610 glass, *Chem. Geol.*, 2003, vol. 197, pp. 111–146.

Stratigrafiya neftegazonosnykh basseinov Sibiri. Rifei i vend Sibirskoi platformy i ee skladchatogo obramleniya (Stratigraphy of Oil and Gas Basins of Siberia. Riphean and Vendian of Siberian Platform and its Fold Framing), Mel'nikov, N.V., Ed., Novosibirsk: Geo, 2005 [in Russian].

Surkov, V.S. and Grishin, M.P. The structure of Riphean sedimentary basins of the Siberian Platform, *Geol. Geofiz.*, 1997, no. 11, pp. 1712–1715.

Tektonika, geodinamika i metallogeniya territorii Respubliki Sakha (Yakutiya) (Tectonics, Geodynamics, and Metallogeny of the Territory of Republic of Sakha (Yakutia)), Parfenov, L.M. and Kuzmin, M.I., Eds., Moscow: MAIK "Nauka/Interperiodika", 2001 [in Russian].

Vernikovsky, V.A., Kotov, A.B., Ponomarchuk, V.A., et al., Late Riphean–Vendian event in the Northern Taimyr evolution: evidence from Sm – Nd, Rb-Sr, and K-Ar dating of the garnet amphibolites of the Stanovoy Ophiolite Belt, *Dokl. Akad. Nauk*, 1997, vol. 352, no. 2, pp. 218–221.

Vernikovsky, V.A., Vernikovskaya, A.E., Pease, V.L., and Gee, D.G., Neoproterozoic orogeny along the margins of Siberia, in *The Neoproterozoic Timanide Orogen of Eastern Baltica*, Gee, D.G. and Pease, V., Eds., *Geol. Soc. London Mem. 30*, 2004, pp. 233–247.

Vernikovsky, V.A. and Vernikovskaya, A.E., Tectonics and evolution of granitoid magmatism in the Yenisei Ridge, *Russ. Geol. Geophys.*, 2006, vol. 47, no. 1, pp. 35–52.

Veselovskii, R.V., Petrov, P.Yu., Karpenko, S.F., et al., New paleomagnetic and isotope data on the Late Proterozoic magmatic complex on the northern slope of the Anabar Uplift, *Dokl. Earth Sci.*, 2006, vol. 410, no. 6, pp. 1–5.

Veselovskii, R.V., Pavlov, V.E., and Petrov, P.Yu., New paleomagnetic data on the Anabar Uplift and the Uchur-Maya Region and their implications for the paleogeography and geological correlation of the Riphean of the Siberian Platform, *Izv., Phys. Solid Earth*, 2009, vol. 45, no. 7, pp. 545–566

Translated by D. Voroschuk